Published in final edited form as:
Science. 2013 November 22; 342(6161): 971–976. doi:10.1126/science.1240537.

The intestinal microbiota modulates the anticancer immune effects of cyclophosphamide

Sophie Viaud[1,3], **Fabiana Saccheri**[1], **Grégoire Mignot**[4,5], **Takahiro Yamazaki**[1], **Romain Daillère**[1,3], **Dalil Hannani**[1], **David P. Enot**[7,8], **Christina Pfirschke**[9], **Camilla Engblom**[9], **Mikael J. Pittet**[9], **Andreas Schlitzer**[10], **Florent Ginhoux**[10], **Lionel Apetoh**[4,5], **Elisabeth Chachaty**[11], **Paul-Louis Woerther**[11], **Gérard Eberl**[12], **Marion Bérard**[13], **Chantal Ecobichon**[14,15], **Dominique Clermont**[16], **Chantal Bizet**[16], **Valérie Gaboriau-Routhiau**[17,18], **Nadine Cerf-Bensussan**[17,18], **Paule Opolon**[19,20], **Nadia Yessaad**[21,22,23,24], **Eric Vivier**[21,22,23,24], **Bernhard Ryffel**[25], **Charles O. Elson**[26], **Joël Doré**[17,27], **Guido Kroemer**[7,8,28,29,30], **Patricia Lepage**[17,27], **Ivo Gomperts Boneca**[14,15], **François Ghiringhelli**[4,5,6,†], and **Laurence Zitvogel**[1,2,3,*,†]

[1]Institut National de la Santé et de la Recherche Médicale, U1015, Equipe labellisée Ligue Nationale Contre le Cancer, Institut Gustave Roussy, Villejuif, France

[2]Centre d'Investigation Clinique Biothérapie CICBT 507, Institut Gustave Roussy, Villejuif, France

[3]Université Paris-Sud, Kremlin Bicêtre, France

[4]Institut National de la Santé et de la Recherche Médicale, U866, Centre Georges François Leclerc, Dijon, France

[5]Institut National de la Santé et de la Recherche Médicale, Group Avenir, Dijon, France

[6]Faculté de Médecine, Université de Bourgogne, Dijon, France

[7]Institut National de la Santé et de la Recherche Médicale, U848, Institut Gustave Roussy, Villejuif, France

[8]Metabolomics and Cell Biology Platforms, Institut Gustave Roussy, Villejuif, France

[9]Center for Systems Biology, Massachusetts General Hospital and Harvard Medical School, Boston, USA

[10]Singapore Immunology Network (SIgN), Agency for Science, Technology and Research (A* STAR), Singapore

[11]Service de Microbiologie, Institut Gustave Roussy, Villejuif, France

[12]Lymphoid Tissue Development Unit, Institut Pasteur, Paris, France

[13]Animalerie Centrale, Institut Pasteur, Paris, France

[14]Institut Pasteur, Unit Biology and genetics of the bacterial cell wall, Paris, France

[15]Institut National de la Santé et de la Recherche Médicale, Group Avenir, Paris, France

[*]Correspondence to: Laurence. ZITVOGEL@gustaveroussy.fr.
[†]Shared senior co-authorship.

The complete set of Materials and Methods is available as supplementary material on *Science* Online.

[16]Institut Pasteur, Collection de l'Institut Pasteur, Paris, France

[17]Institut National de la Recherche Agronomique, Micalis - UMR1319, 78350 Jouy-en-Josas, France

[18]Institut National de la Santé et de la Recherche Médicale U989, Université Paris Descartes, 75730 Paris, France

[19]Institut Gustave Roussy, IFR54, Villejuif, France

[20]Institut Gustave Roussy, IRCIV, Laboratoire de Pathologie Expérimentale, Villejuif, France

[21]Centre d'Immunologie de Marseille-Luminy, Aix-Marseille Université UM2, Marseille, France

[22]Institut National de la Santé et de la Recherche Médicale, UMR 1104, Marseille, France

[23]Centre National de la Recherche Scientifique, Unité Mixte de Recherche 7280, Marseille, France

[24]Assistance Publique des Hôpitaux de Marseille, Hôpital de la Conception, Marseille, France

[25]Laboratory of Molecular and Experimental Immunology and Neurogenetics, UMR 7355, CNRS-University of Orleans, Orleans, France

[26]University of Alabama at Birmingham, Birmingham, AL, USA

[27]AgroParisTech, Micalis - UMR1319, 78352 Jouy-en-Josas, France

[28]Equipe 11 labellisée Ligue contre le Cancer, Centre de Recherche des Cordeliers, Paris, France

[29]Pôle de Biologie, Hôpital Européen Georges Pompidou, Assistance Publique–Hôpitaux de Paris, Paris, France

[30]Université Paris Descartes, Paris, France

Abstract

Cyclophosphamide is one of several clinically important cancer drugs whose therapeutic efficacy is due in part to their ability to stimulate anti-tumor immune responses. Studying mouse models, we demonstrate that cyclophosphamide alters the composition of microbiota in the small intestine and induces the translocation of selected species of $Gram^+$ bacteria into secondary lymphoid organs. There, these bacteria stimulate the generation of a specific subset of "pathogenic" T helper 17 (pTh17) cells and memory Th1 immune responses. Tumor-bearing mice that were germ-free or that had been treated with antibiotics to kill $Gram^+$ bacteria showed a reduction in pTh17 responses and their tumors were resistant to cyclophosphamide. Adoptive transfer of pTh17 cells partially restored the anti-tumor efficacy of cyclophosphamide. These results suggest that the gut microbiota help shape the anticancer immune response.

It is now well established that gut commensal bacteria profoundly shape mammalian immunity (1). Intestinal dysbiosis, which constitutes a disequilibrium in the bacterial ecosystem, can lead to overrepresentation of some bacteria able to promote colon carcinogenesis by favoring chronic inflammation or local immunosuppression (2, 3).

However, the effects of microbial dysbiosis on non-gastrointestinal cancers are unknown. Anticancer chemotherapeutics often cause mucositis (a debilitating mucosal barrier injury associated with bacterial translocation) and neutropenia, two complications that require treatment with antibiotics, which in turn can result in dysbiosis (4, 5). Some antineoplastic agents mediate part of their anticancer activity by stimulating anticancer immune responses (6). Cyclophosphamide (CTX), a prominent alkylating anticancer agent induces immunogenic cancer cell death (7, 8), subverts immunosuppressive T cells (9) and promotes Th1 and Th17 cells controlling cancer outgrowth (10). Here, we investigated the impact of CTX on the small intestine microbiota and its ensuing effects on the antitumor immune response.

We characterized the inflammatory status of the gut epithelial barrier 48 hours following therapy with non-myeloablative doses of CTX or the anthracycline doxorubicin in naive mice. Both drugs caused shortening of small intestinal villi, discontinuities of the epithelial barrier, interstitial edema and focal accumulation of mononuclear cells in the lamina propria (LP) (Fig. 1A–B). Post-chemotherapy, the numbers of goblet cells and Paneth cells were increased in villi (Fig. 1C) and crypts (Fig. 1D) respectively. The antibacterial enzyme lysozyme (but not the microbiocide peptide RegIIIγ) was upregulated in the duodenum of CTX-treated mice (Fig. 1E). Orally administered fluorescein isothiocyanate (FITC)-dextran became detectable in the blood (11) 18 h post CTX, confirming an increase in intestinal permeability (Fig. 1F). Disruption of the intestinal barrier was accompanied by a significant translocation of commensal bacteria in >50% mice into mesenteric lymph nodes and spleens that was well detectable 48 h post-CTX, less so after doxorubicin treatment (Fig. 2A). Several Gram$^+$ bacterial species, including *Lactobacillus johnsonii* (growing in >40% cases), *Lactobacillus murinus* and *Enterococcus hirae*, could be cultured from these lymphoid organs (Fig. 2B).

Next, we analyzed the overall composition of the gut microbiota by high-throughput 454 pyrosequencing, followed by quantitative PCR targeting the domain bacteria and specific bacterial groups. Although CTX failed to cause a major dysbiosis at early time points (24–48h, Fig. S1), CTX significantly altered the microbial composition of the small intestine (but not of the caecum) in mice bearing subcutaneous cancers (namely metastasizing B16F10 melanomas and non-metastasizing MCA205 sarcomas) one week after its administration (Fig. 2C, Fig. S2). Consistent with previous reports on fecal samples from patients (12), CTX induced a reduction of bacterial species of the *Firmicutes* phylum (Fig. S2) distributed within four genera and groups (*Clostridium* cluster *XIVa, Roseburia, unclassified Lachnospiraceae*, *Coprococcus*, Table S1) in the mucosa of CTX-treated animals. Quantitative PCR was applied to determine the relative abundance (as compared to all bacteria) of targeted groups of bacteria (*Lactobacillus*, *Enterococcus*, cluster IV of the *Clostridium leptum* group) in the small intestine mucosa from CTX versus vehicle-treated naïve and tumor-bearing mice. In tumor bearers, the total bacterial load of the small intestine at 7 days post-CTX as well as the bacterial counts of the *Clostridium leptum* were not affected (Fig. 2D). However, CTX treatment led to a reduction in the abundance of lactobacilli and enterococci (Fig. 2D). Altogether, these data reveal the capacity of CTX to

provoke the selective translocation of distinct Gram$^+$ bacterial species followed by significant changes in the small intestinal microbiome.

Coinciding with dysbiosis 7 days post-CTX, the frequencies of CD103$^+$CD11b$^+$ dendritic cells (Fig. S3A) and TCRαβ $^+$CD3$^+$ T cells expressing the transcription factor RORγt (Fig. S3B) were significantly decreased in the lamina propria (LP) of the small intestine (but not the colon), as revealed by flow cytometry of dissociated tissues (Fig. S3B) and *in situ* immunofluorescence staining (Fig. S3C). RORγt is required for the generation of Th17 cells (which produce interleukin-17, IL-17), and strong links between gut-residing and systemic Th17 responses have been established in the context of autoimmune diseases affecting joints, the brain or the pancreas (13–15). Confirming previous work (9, 10), CTX induced the polarization of splenic CD4$^+$ T cells towards a Th1 (interferon-γ [IFNγ]-producing) and Th17 pattern (Fig. 3A, Fig. S3D). This effect was specific for CTX and was not found for doxorubicin (Fig. S4). The gut microbiota was indispensable for gearing the conversion of naïve CD4$^+$T cells into IL-17 producers in response to CTX. Indeed, the *ex vivo* IL-17 release by TCR-stimulated splenocytes increased upon CTX treatment of specific pathogen-free (SPF) mice, yet failed to do so in germ-free (GF) mice (Fig. 3A, left panel). Sterilization of the gut by broad-spectrum antibiotics (ATB, a combination of colistin, ampicillin and streptomycin, Fig. S5) also suppressed the CTX-stimulated secretion of IL-17 (Fig. 3A, right panel) and IFNγ by TCR-stimulated splenocytes (Fig. S3D). Treatment of mice with vancomycin, an antibiotic specific for Gram$^+$ bacteria (16), also reduced the CTX-induced Th17 conversion (Fig. 3A, right panel). In conventional SPF mice, the counts of lactobacilli and SFB measured in small intestine mucosa (Fig. 2D) positively correlated with the Th1 and Th17 polarization of splenocytes (Fig. 3B, Fig. S3E) whereas that of *Clostridium* group IV did not (Fig. 3B). Altogether, these results point to a specific association between particular microbial components present in the gut lumen (and occasionally in lymphoid organs) and the polarity of Th responses induced by CTX treatment.

CTX increased the frequency of “pathogenic “Th17 (pTh17) cells, which share hallmarks of Th1 cells (nuclear expression of the transcription factor T-bet, cytoplasmic expression of IFNγ and surface exposure of the chemokine receptor CXCR3) and Th17 cells (expression of RORγt, IL-17 and CCR6) (17, 18), within the spleen (Fig. S3F, Fig. 3C). Again, this response depended on the gut microbiota (Fig. 3C). Moreover, the increase in pTh17 cells required expression of myeloid differentiation primary response gene 88 (MyD88), which signals downstream of toll-like receptors (Fig. S6A) and is required for the therapeutic success of anticancer chemotherapies in several tumor models (19). In contrast, the two pattern recognition receptors, nucleotide-binding oligomerization domain-containing (Nod)1 and Nod2, were dispensable for the CTX-induced raise in splenic pTh17 cells and for the tumor growth retarding effects of CTX (Fig. S6B). These results establish the capacity of CTX to stimulate pTh17 cells through a complex circuitry that involves intestinal bacteria and MyD88, correlating with its anticancer effects. Beyond its general effect on the frequency of pTh17 cells, CTX induced TCR-restricted, antigen specific immune responses against commensal bacteria (Fig. S7). Hence, we addressed whether Gram$^+$ bacterial species that translocated into secondary lymphoid organs in response to CTX (Fig. 2A) could

polarize naïve $CD4^+$ T cells towards a Th1 or Th17 pattern. Both *L. johnsonii* and *E. hirae* stimulated the differentiation of naïve $CD4^+$ T cells into Th1 and Th17 cells *in vitro*, in the presence of bone marrow-derived dendritic cells, while toll-like receptor 4-activating purified bacterial lipopolysaccharide (LPS) or *E. coli* both had a minor effect (Fig. S8). Moreover, orally fed *L. johnsonii* and *E. hirae* but neither *L. plantarum* (a bacterium that was not detected in translocation experiments, Fig. 2B) nor *L. reuteri* facilitated the reconstitution of the pool of pTh17 cells in the spleen of ATB-treated SPF mice (Fig. 3D). Th1 memory responses against *L. johnsonii* were consistently detected in 50% of mice receiving CTX (Fig. 3E) but not in control mice, after *in vitro* restimulation of $CD4^+$T cells with bone marrow-derived dendritic cells loaded with *L. johnsonii* (and to a lesser extent *E. hirae*, but not with other commensals or pathobionts). Taking into account that CTX-induced dysbiosis peaks at late time points (day 7), we postulate that the translocation of a specific set of $Gram^+$ commensal bacteria is necessary and sufficient to mediate the CTX-driven accumulation of pTh17 cells and Th1 bacteria- specific memory T cell responses.

Because commensal bacteria modulate intestinal and systemic immunity post-CTX, we further investigated the effect of antibiotics on CTX-mediated tumor growth inhibition. Long-term treatment with broad-spectrum ATB reduced the capacity of CTX to cure P815 mastocytomas established in syngenic DBA2 mice (Fig. 4A, Fig. S9A). Moreover, the antitumor effects mediated by CTX against MCA205 sarcomas were reduced in GF compared with SPF mice (Fig. 4B, left and middle panels). Driven by the observations that CTX mostly induced the translocation of $Gram^+$ bacteria and that $Gram^+$ bacteria correlated with splenic Th1/Th17 polarization, we compared the capacity of several ATB regimens, namely vancomycin (depleting $Gram^+$ bacteria) and colistin (depleting most $Gram^-$ bacteria) to interfere with the tumor growth-inhibitory effects of CTX. Vancomycin, and to a lesser extent colistin compromised the anti-tumor efficacy of CTX against MCA205 sarcoma (Fig. 4C, Fig. S9B). Using a transgenic tumor model of autochthonous lung carcinogenesis driven by oncogenic K-Ras coupled to conditional p53 deletion (20), we confirmed the inhibitory role of vancomycin on the anticancer efficacy of a CTX-based chemotherapeutic regimen (Fig. 4D). Vancomycin also prevented the CTX-induced accumulation of pTh17 in the spleen (Fig. 4E) and reduced the frequencies of tumor-infiltrating $CD3^+$ T cells and Th1 cells (Fig. 4F).

Although the feces of most SPF mice treated with ATB usually were free of cultivable bacteria (Fig. S5), some mice occasionally experienced the outgrowth of *Parabacteroides distasonis*, a species reported to maintain part of the intestinal regulatory T cell repertoire and to mediate local anti-inflammatory effects (21–23). This bacterial contamination was associated with the failure of an immunogenic chemotherapy (doxorubicin) against established MCA205 sarcomas (Fig. S10A). Moreover, experimental recolonization of ATB-sterilized mice with *P. distasonis* compromised the anticancer effects of doxorubicin (Fig. S10B), demonstrating that gut microbial dysbiosis abrogates anticancer therapy. Finally, monoassociation of tumor-bearing GF mice with SFB, which promotes Th17 cell differentiation in the LP (1, 13, 14) also had a detrimental impact on the tumor growth-inhibitory effect of CTX (Fig. 4B, right panel).

The aforementioned results highlight the association between specific CTX-induced alterations in gut microbiota, the accumulation of pTh17 cells in the spleen and the success of chemotherapy. To establish a direct causal link between these phenomena, we adoptively transferred Th17 or pTh17 populations into vancomycin-treated mice and evaluated their capacity to reestablish the CTX-mediated tumor growth retardation. *Ex vivo* propagated pTh17 exhibited a pattern of gene expression similar to that expressed by CTX-induced splenic $CD4^+$ T cells *in vivo* (Fig. S11). Only pTh17 but not Th17 cells were able to rescue the negative impact of vancomycin on the CTX-mediated therapeutic effect (Fig. 4G). These results emphasize the importance of pTh17 cells for CTX-mediated anticancer immune responses.

Although much of the detailed molecular mechanisms governing the complex interplay between epithelial cells, gut microbiota and intestinal immunity remain to be deciphered, the present study unveils the unsuspected impact of the intestinal flora on chemotherapy-elicited anticancer immune responses. Our data underscore new risks associated with antibiotic medication during cancer treatments as well as the potential therapeutic utility of manipulating the gut microbiota.

Supplementary Material

Refer to Web version on PubMed Central for supplementary material.

Acknowledgments

We thank Thierry Angélique (Institut Pasteur), Caroline Flament, Marie Vétizou (Gustave Roussy) and Karine LeRoux (INRA) for their excellent work. The data reported in this manuscript are tabulated in the main paper and in the supplementary materials. This work was supported by Institut National du Cancer (INCa), la Ligue contre le cancer (LIGUE labellisée, LZ, GK), SIRIC Socrates, LABEX and PACRI Onco-Immunology, European Research Council Advanced Grant (to GK), European Research Council starting grant (PGNfromSHAPEtoVIR n°202283 to IGB) and partially supported by NIH grant P01DK071176 (C O. E).

References and Notes

1. Hooper LV, Littman DR, Macpherson AJ. Interactions between the microbiota and the immune system. Science. 2012 Jun 8.336:1268. [PubMed: 22674334]
2. Grivennikov SI, et al. Adenoma-linked barrier defects and microbial products drive IL-23/IL-17-mediated tumour growth. Nature. 2012 Nov 8.491:254. [PubMed: 23034650]
3. Wu S, et al. A human colonic commensal promotes colon tumorigenesis via activation of T helper type 17 T cell responses. Nat Med. 2009 Sep.15:1016. [PubMed: 19701202]
4. van Vliet MJ, Harmsen HJ, de Bont ES, Tissing WJ. The role of intestinal microbiota in the development and severity of chemotherapy-induced mucositis. PLoS Pathog. 2010 May. 6:e1000879. [PubMed: 20523891]
5. Ubeda C, et al. Vancomycin-resistant Enterococcus domination of intestinal microbiota is enabled by antibiotic treatment in mice and precedes bloodstream invasion in humans. J Clin Invest. 2010 Dec.120:4332. [PubMed: 21099116]
6. Kroemer G, Galluzzi L, Kepp O, Zitvogel L. Immunogenic cell death in cancer therapy. Annu Rev Immunol. 2013 Nov 12.31:51. [PubMed: 23157435]
7. Sistigu A, et al. Immunomodulatory effects of cyclophosphamide and implementations for vaccine design. Semin Immunopathol. 2011 Jul.33:369. [PubMed: 21611872]

8. Schiavoni G, et al. Cyclophosphamide synergizes with type I interferons through systemic dendritic cell reactivation and induction of immunogenic tumor apoptosis. Cancer Res. 2011 Feb 1.71:768. [PubMed: 21156650]
9. Ghiringhelli F, et al. CD4+CD25+ regulatory T cells suppress tumor immunity but are sensitive to cyclophosphamide which allows immunotherapy of established tumors to be curative. Eur J Immunol. 2004 Feb.34:336. [PubMed: 14768038]
10. Viaud S, et al. Cyclophosphamide induces differentiation of Th17 cells in cancer patients. Cancer Res. 2011 Feb 1.71:661. [PubMed: 21148486]
11. Yang J, Liu KX, Qu JM, Wang XD. The changes induced by cyclophosphamide in intestinal barrier and microflora in mice. European journal of pharmacology. 2013 Aug 15.714:120. [PubMed: 23791611]
12. Zwielehner J, et al. Changes in human fecal microbiota due to chemotherapy analyzed by TaqMan-PCR, 454 sequencing and PCR-DGGE fingerprinting. PLoS One. 2011; 6:e28654. [PubMed: 22194876]
13. Wu HJ, et al. Gut-residing segmented filamentous bacteria drive autoimmune arthritis via T helper 17 cells. Immunity. 2010 Jun 25.32:815. [PubMed: 20620945]
14. Lee YK, Menezes JS, Umesaki Y, Mazmanian SK. Proinflammatory T-cell responses to gut microbiota promote experimental autoimmune encephalomyelitis. Proc Natl Acad Sci U S A. 2011 Mar 15.108(Suppl 1):4615. [PubMed: 20660719]
15. Wen L, et al. Innate immunity and intestinal microbiota in the development of Type 1 diabetes. Nature. 2008 Oct 23.455:1109. [PubMed: 18806780]
16. Rice LB. Antimicrobial resistance in gram-positive bacteria. American journal of infection control. 2006 Jun.34:S11. [PubMed: 16813977]
17. Lee Y, et al. Induction and molecular signature of pathogenic TH17 cells. Nat Immunol. 2012 Oct. 13:991. [PubMed: 22961052]
18. Ghoreschi K, et al. Generation of pathogenic T(H)17 cells in the absence of TGF-beta signalling. Nature. 2010 Oct 21.467:967. [PubMed: 20962846]
19. Apetoh L, et al. Toll-like receptor 4-dependent contribution of the immune system to anticancer chemotherapy and radiotherapy. Nat Med. 2007 Sep.13:1050. [PubMed: 17704786]
20. Cortez-Retamozo V, et al. Origins of tumor-associated macrophages and neutrophils. Proc Natl Acad Sci U S A. 2012 Feb 14.109:2491. [PubMed: 22308361]
21. Kverka M, et al. Oral administration of Parabacteroides distasonis antigens attenuates experimental murine colitis through modulation of immunity and microbiota composition. Clin Exp Immunol. 2011 Feb.163:250. [PubMed: 21087444]
22. Lathrop SK, et al. Peripheral education of the immune system by colonic commensal microbiota. Nature. 2011 Oct 13.478:250. [PubMed: 21937990]
23. Geuking MB, et al. Intestinal bacterial colonization induces mutualistic regulatory T cell responses. Immunity. 2011 May 27.34:794. [PubMed: 21596591]

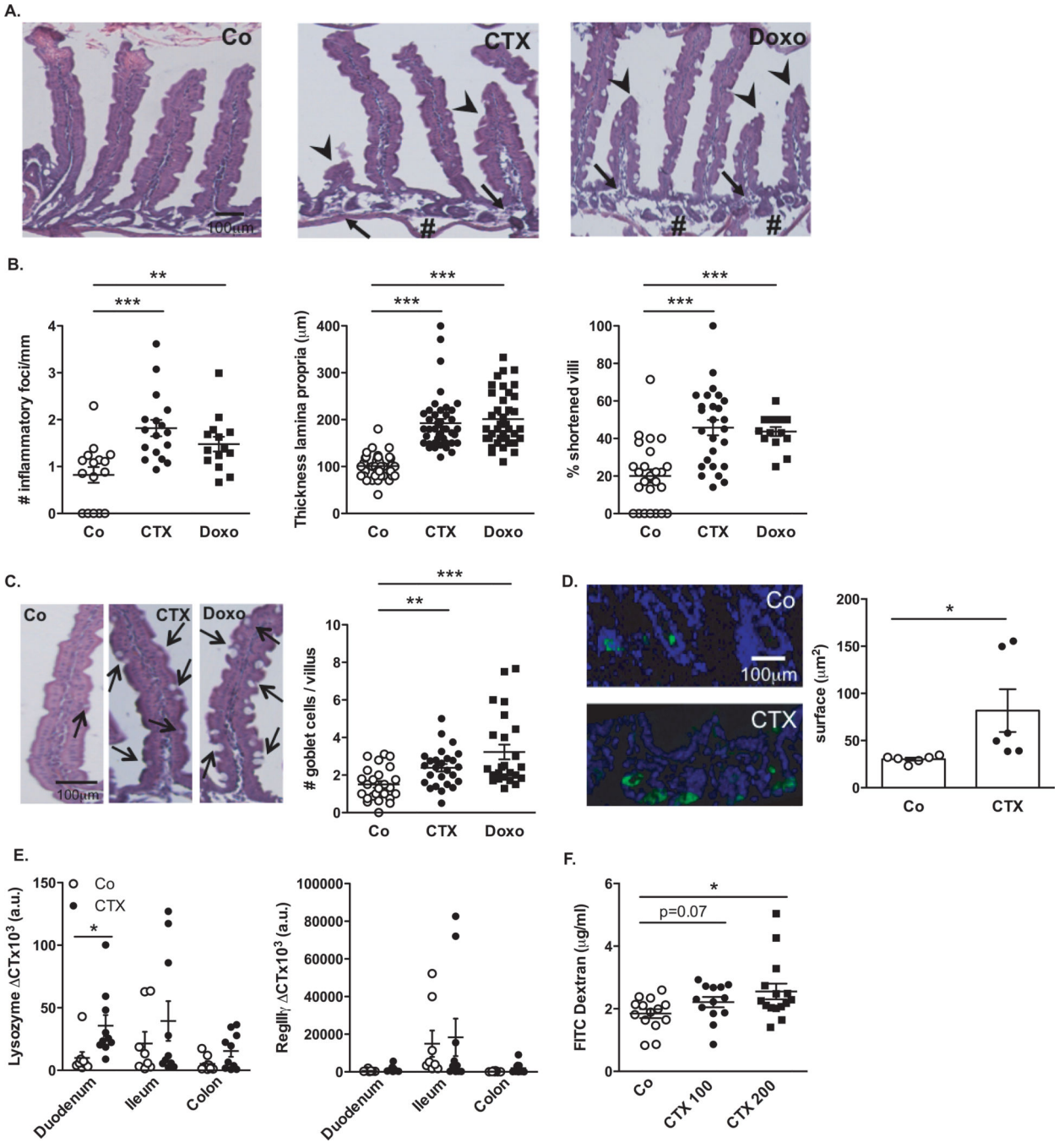

Fig. 1. Cyclophosphamide disrupts gut mucosal integrity

(**A–B**). Hematoxilin-eosin staining of the small intestine epithelium at 48h post-NaCl (Co) or CTX or doxorubicin (Doxo) therapy in C57BL/6 naïve mice (A). The numbers of inflammatory foci depicted/mm (B, left panel, indicated with arrowhead on A), thickness of the lamina propria reflecting edema (B, middle panel, indicated with # on A) and the reduced length of villi (B, right panel, indicated with arrowhead in A) were measured in 5 ilea on 100 villi/ileum from CTX or Doxo -treated mice. (**C**). A representative microphotograph of an ileal villus containing typical mucin-containing goblet cells is shown

in vehicle- and CTX or Doxo-treated mice (left panels). The number of goblet cells/villus was enumerated in the right panel for both chemotherapy agents. (**D**). Specific staining of Paneth cells is shown in two representative immunofluorescence microphotographs (D, left panels). The quantification of Paneth cells was performed measuring the average area of the lysozyme-positive clusters in 6 ilea harvested from mice treated with NaCl (Co) or CTX at 24–48 hours. **(E)**. Quantitative PCR (qPCR) analyses of Lysozyme M and RegIIIγ transcription levels in duodenum and ileum lamina propria cells from mice treated with CTX at 18 hours. Means±SEM of normalized deltaCT of 3–4 mice/group concatenated from three independent experiments. **(F)**. *In vivo* intestinal permeability assays measuring 4 kDa fluorescein isothiocyanate (FITC)-dextran plasma accumulation at 18 hours post-CTX at two doses. Graph showing all data from four independent experiments, each dot representing one mouse (n=13–15). Data were analyzed with the t-test. *, $p<0.05$, **, $p<0.01$, ***, $p<0.001$.

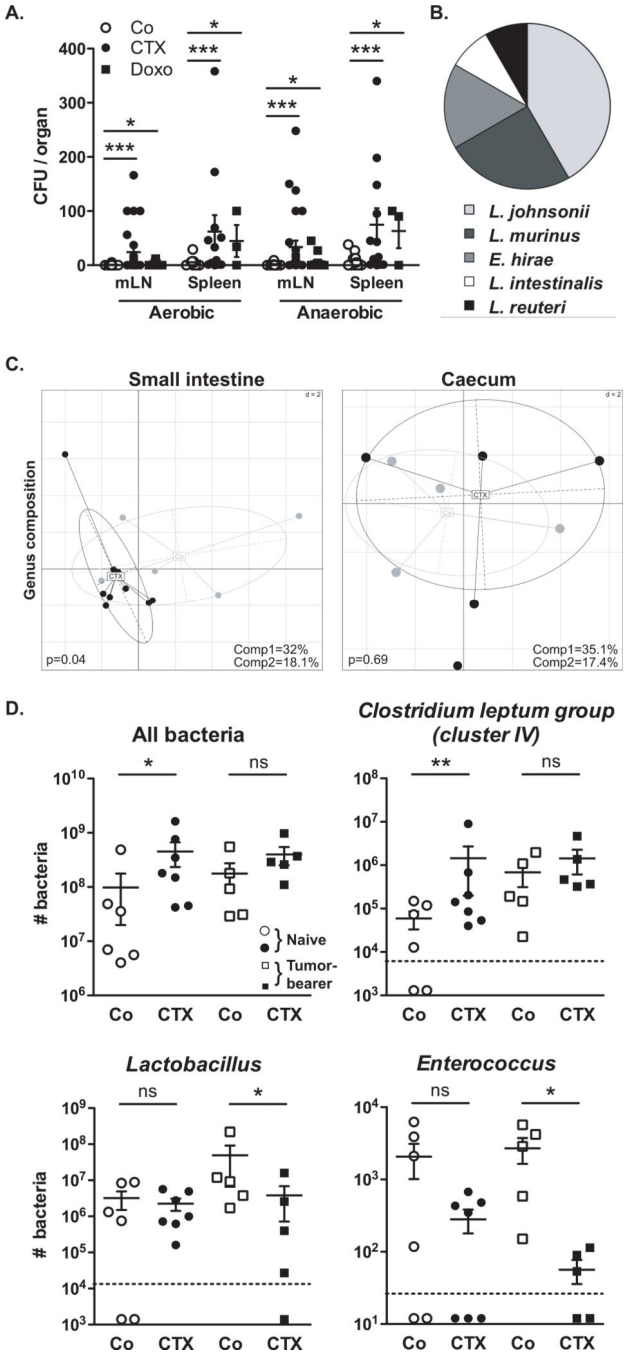

Fig. 2. Cyclophosphamide induces mucosa-associated microbial dysbiosis and bacterial translocation in secondary lymphoid organs

(**A–B)**. At 48 hours post-CTX or Doxo, mesenteric lymph node (mLN) and spleen cells from naïve mice were cultivated in aerobic and anaerobic conditions and colonies were enumerated (A) from each mouse treated with NaCl (Co) (n=10–16), CTX (n=12–27) or Doxo (n=3–17) (3–4 experiments) and identified by mass spectrometry (B). In NaCl controls, attempts of bacterial identification mostly failed and yielded 67% *L. murinus* (not shown). Data were analyzed with the t-test. (**C**). The microbial composition (genus level)

was analyzed by 454 pyrosequencing of the 16S rRNA gene from ilea and caeca of naïve mice and B16F10 tumor bearers. Principal Component Analyses (PCA) highlighted specific clustering of mice microbiota (each dot represents one mouse) depending on the treatment (NaCl: Co, grey dots; CTX-treated, black dots). A Monte Carlo rank test was applied to assess the significance of these clusterings. (**D**). Quantitative PCR (qPCR) analyses of various bacterial groups associated with small intestine mucosa were performed on CTX or NaCl (Co)-treated, naïve or MCA205 tumor-bearing mice. Absolute values were calculated for total bacteria, *Lactobacilli*, *Enterococci* and *Clostridium* group IV and normalized by the dilution and weight of the sample. Standard curves were generated from serial dilutions of a known concentration of genomic DNA from each bacterial group and by plotting threshold cycles (Ct) vs bacterial quantity (CFU). Points below the dotted lines were under the detection threshold. Data were analyzed with the linear model or generalized linear model. *, $p<0.5$, **, $p<0.1$, ***, $p<0.001$, ns, non significant.

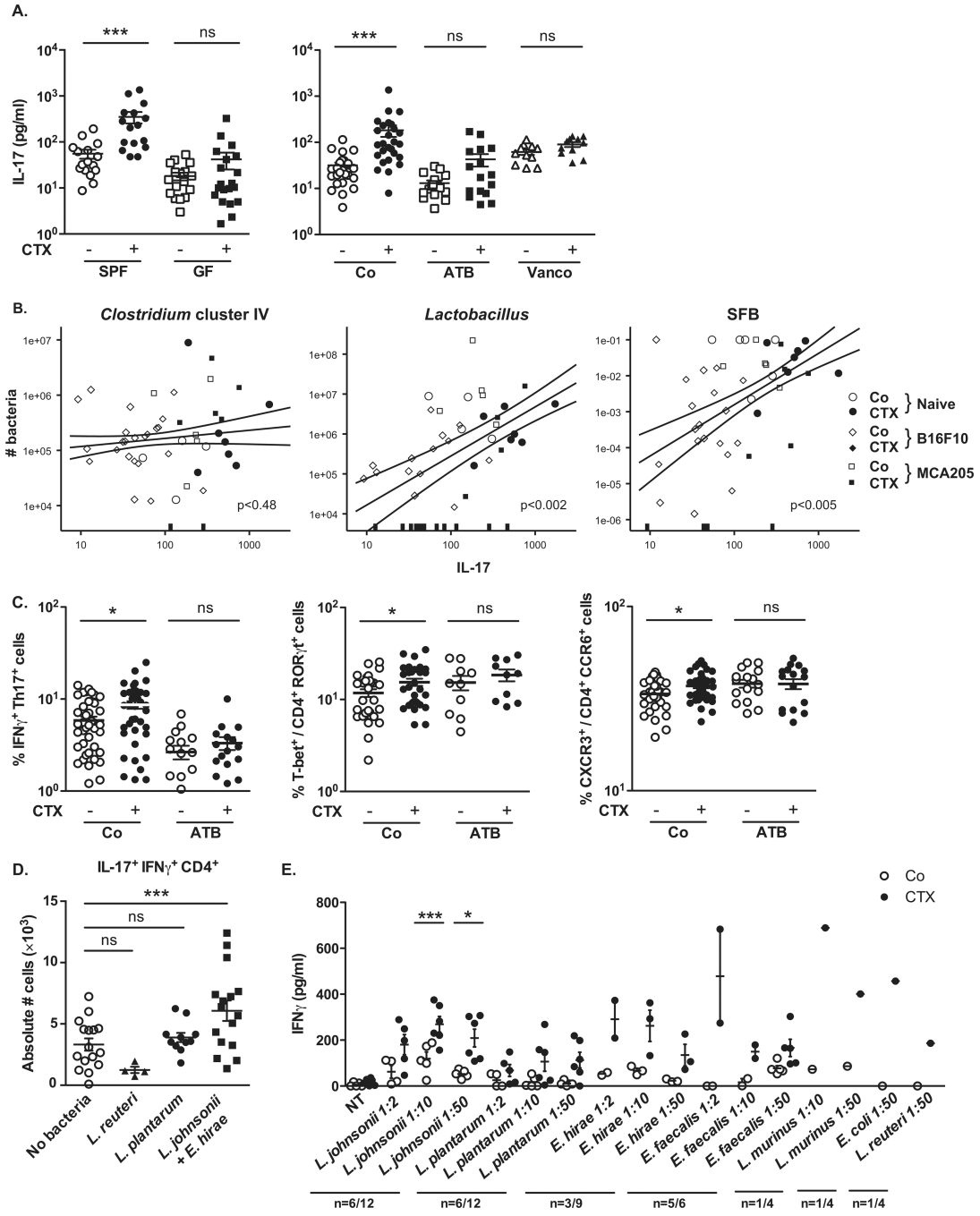

Fig. 3. CTX-induced pTh17 effectors and memory Th1 responses depend on gut microbiota

A). Splenocytes from CTX versus NaCl treated animals reared in germ-free (GF) or conventional specific pathogen-free (SPF) conditions (left panel) and treated or not with ATB or vancomycin (Vanco) (right panel) were cross-linked using anti-CD3+anti-CD28 Ab for 48h. IL-17 was measured by ELISA. Two to 3 experiments containing 2–9 mice/group are presented, each dot representing one mouse. (**B**). Correlations between the quantity of specific mucosal bacterial groups and the spleen Th17 signature. Each dot represents one mouse bearing no tumor (round dots), a B16F10 melanoma (diamond dots) or a MCA205

sarcoma (square dots), open dots featuring NaCl-treated mice and full dots indicating CTX-treated animals. (**C**). Intracellular analyses of splenocytes harvested from non-tumor-bearing mice after 7 days of either NaCl or CTX treatment, under ATB or water regimen as control. Means±SEM of percentages of IFNγ^+ Th17 cells, T-bet$^+$ cells among RORγt$^+$ CD4$^+$ T cells and CXCR3$^+$ cells among CCR6$^+$CD4$^+$ T cells in 2 – 8 independent experiments, each dot representing one mouse. (**D**) Intracellular staining of total splenocytes harvested 7 days post-CTX treatment from naïve mice orally-reconstituted with the indicated bacterial species after ATB treatment. (**E**). 7 days post CTX or NaCl (Co) treatment, splenic CD4$^+$ T cells were restimulated *ex vivo* with bone-marrow dendritic cells (BM-DCs) loaded with decreasing amounts of bacteria for 24 hours. IFNγ release, monitored by ELISA is shown. The numbers of responder mice (based on the NaCl baseline threshold) out of the total number of mice tested is indicated (n). Statistical comparisons were based on the paired t-test. Data were either analyzed with beta regression or linear model and correlation analyses from modified Kendall tau. *, $p<0.05$, ***, $p<0.001$, ns, non significant.

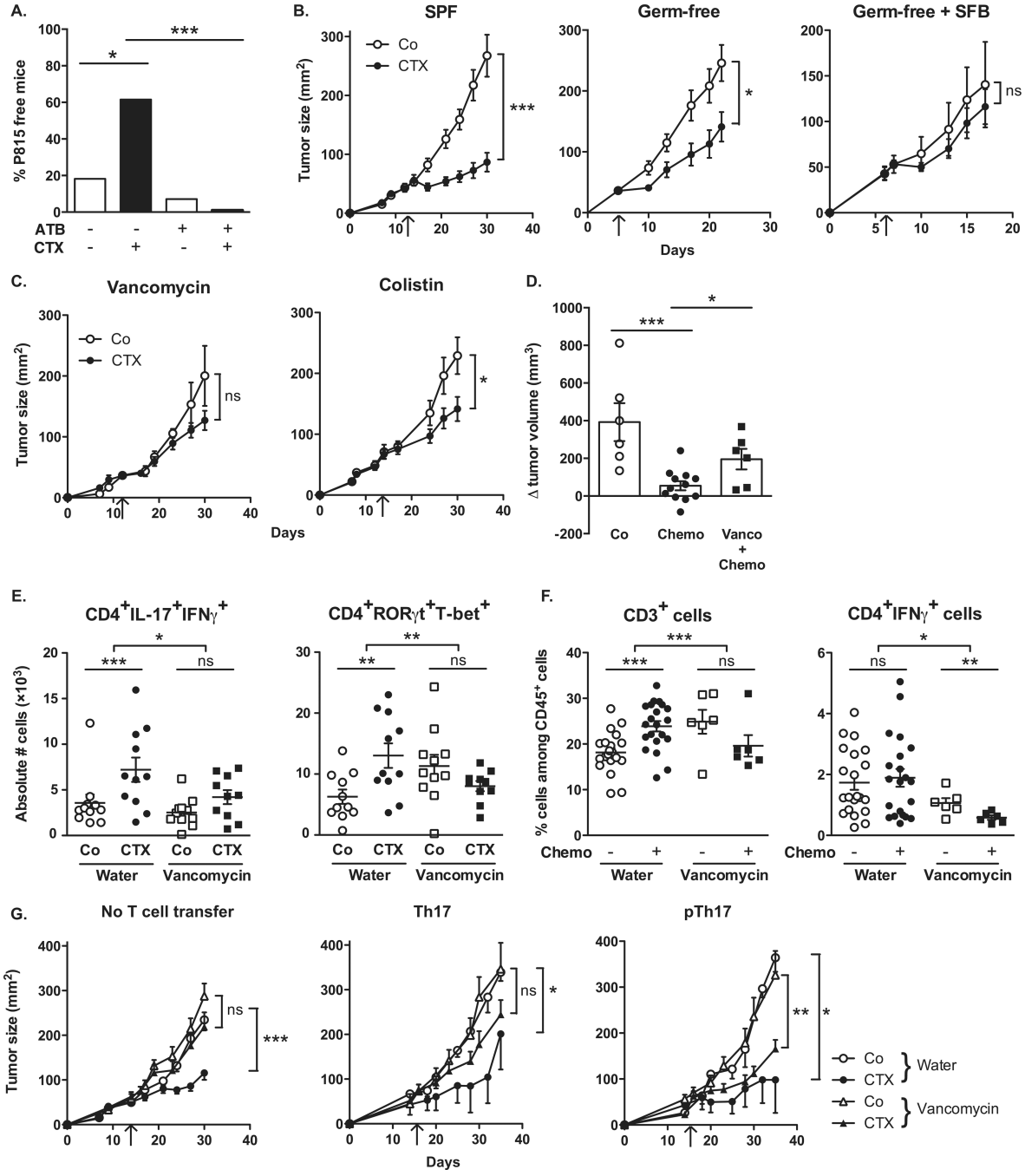

Fig. 4. Vancomycin blunts CTX-induced pTh17 differentiation which is mandatory for the tumoricidal activity of chemotherapy

(A). After a 3 week-long pretreatment with broad-spectrum ATB, DBA2 mice were inoculated with P815 mastocytomas (day 0), treated at day 6 with CTX (arrow) and tumor growth was monitored. Tumor growth kinetics are shown in Fig. S9A and percentages of tumor-free mice at sacrifice are depicted for two experiments of 11–14 mice/group. (B). MCA205 sarcoma were inoculated at day 0 in specific pathogen-free (SPF) or germ-free (GF) mice that were optionally mono-associated with segmented filamentous bacteria (SFB), treated with CTX (arrow) and monitored for growth kinetics (means±SEM). One

representative experiment (n=5–8 mice/group) out of two to three is shown for GF mice and two pooled experiments (n=14 mice/group) for SPF mice (C). After a 3 week- conditioning with vancomycin or colistin, C57BL/6 mice were inoculated with MCA205 sarcomas (day 0), treated at day 12–15 with CTX (arrow) and tumor growth was monitored. Concatenated data (n=15–20 mice/group) from two independent experiments are shown for colistin treatment and one representative experiment (n=6 mice/group) for vancomycin treatment. (D). Eight week-old KP (*KrasLSL*-G12D/WT; $p53^{Flox/Flox)}$ mice received an adenovirus expressing the Cre recombinase (AdCre) by intranasal instillation to initiate lung adenocarcinoma (d0). Vancomycin was started for a subgroup of mice (“Chemo + Vanco”) on d77 post-AdCre. One week after the start of vancomycin, CTX-based chemotherapy was applied i.p. to mice that only received chemotherapy (“Chemo”) or those that received in parallel vancomycin (“Chemo + Vanco”). Mice received chemotherapy on d84, d91 and d98. A control group was left untreated ("Co"). Data show the evolution of total lung tumor volumes (mean±SEM) assessed by non invasive imaging between d73 and d100 in 6–12 mice/group. (E). As in Fig. 3C, we determined the number of pTh17 cells in spleens from untreated or vancomycin treated mice bearing established (15–17 days) MCA205 tumors, 7 days after CTX treatment. Each dot represents one mouse from 2 pooled experiments. (F). Flow cytometric analyses of $CD3^+$ and $CD4^+IFN\gamma^+$ T cells were performed by gating on $CD45^+$ live tumor-infiltrating lymphocytes (TILs) extracted from day 18 established MCA205 tumors (8 days post-CTX) in water or vancomycin-treated mice. Each dot representing one mouse from up to four pooled experiments. (G). MCA205 tumors established in WT mice pretreated for 3 weeks with water or vancomycin were injected with CTX (arrow), and tumor growth was monitored. At day 7 post-CTX, 3 million of *ex vivo* generated Th17 or pTh17 $CD4^+$ T cells were injected intravenously. Up to three experiments comprising 2–10 mice/group were pooled. Data were either analyzed with the t-test, linear model or generalized linear model. *, $p<0.5$, **, $p<0.1$, ***, $p<0.001$, ns, non significant.